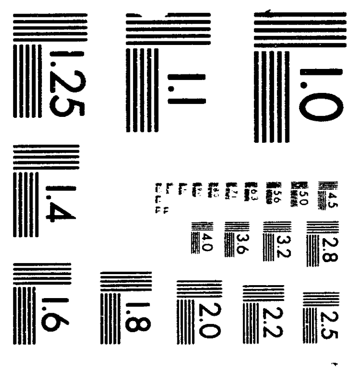
1.0
1.1
1.25
1.4
1.6
1.8
2.0
2.2
2.5
2.8
3.2
3.6
4.0
4.5
5.0
5.6

Conf-930928--19

PNL-SA-22456

RELATIONSHIP BETWEEN SWELLING AND IRRADIATION CREEP IN COLD-WORKED PCS STAINLESS STEEL IRRADIATED TO ~178 DPA AT ~400°C

M. B. Toloczko[a]
F. A. Garner

September - October 1993

Presented at the
Sixth International Conference on
Fusion Reactor Materials
September 27 - October 1, 1993
Stressa, Italy

Work supported by
the U.S. Department of Energy
under Contract DE-AC06-76RLO 1830

Pacific Northwest Laboratory
Richland, Washington 99352

(a) University of California
Santa Barbara, California

RELATIONSHIP BETWEEN SWELLING AND IRRADIATION CREEP IN COLD-WORKED PCA STAINLESS STEEL IRRADIATED TO ~178 DPA AT ~400° C.

M.B. Toloczko[1] and F.A. Garner[2]

1. Department of Chemical and Nuclear Engineering, University of California, Santa Barbara CA, 93106, USA
2. Pacific Northwest Laboratory, Richland WA, 99352, USA

ABSTRACT

The eighth and final irradiation segment for pressurized tubes constructed from the fusion Prime Candidate Alloy (PCA) has been completed in FFTF. At 178 dpa and ~400°C, the irradiation creep of 20% cold-worked PCA has become dominated by the "creep disappearance" phenomenon. The total diametral deformation rate has reached the limiting value of 0.33%/dpa at the three highest stress levels employed in this test. The stress-enhancement of swelling tends to camouflage the onset of creep disappearance, however, requiring the use of several non-traditional techniques to extract the creep coefficients. No failures occurred in these tubes, even though the swelling ranged from ~20 to ~40%.

Phone: 509-376-4136 Fax: 509-376-0418 (F. A. Garner)

INTRODUCTION

Data are required on the response to stress of structural alloys during irradiation in fusion power devices. A large amount of creep data has been generated in fission reactors at stress levels that are usually greater than the intended stress range envisioned in the fusion environment. Some translation of the data are, therefore, required to accommodate the spectral and stress range differences between the two environments (1). One material of particular interest is the austenitic Prime Candidate Alloy (PCA) whose composition is Fe-16.6Ni-14.3Cr-1.95Mo-1.83Mn-0.31Ti-0.52Si-0.048C-0.014P-0.025S-0.04V-0.02Nb-0.04Co-0.02Cu-0.05Al-0.001B-0.008N.

EXPERIMENTAL DETAILS

Helium pressurized tubes constructed from the PCA fusion heat K280 in the 20% cold-worked condition have completed their eighth irradiation segment in FFTF/MOTA[1] at a nominal temperature of ~400°C. These 2.24 cm long tubes were periodically discharged from reactor and, prior to reinsertion into reactor, measurements were made of their diameter using laser profilometry (2). These tubes were inserted in all MOTA vehicles from MOTA-1A through MOTA-1G and then continued into MOTA-2B. The initial hoop stress levels were 0, 30, 60, 100, 140 and 200 MPa. Table 1 presents the detailed temperature history of these tubes, which reached dpa levels as large as ~178 dpa. Irradiation temperatures varied somewhat from one MOTA to the next, but during any one irradiation interval, the temperature was actively controlled within ±5°C of the nominal

1 Fast Flux Test Facility/Materials Open Test Assembly

temperature. The strains of these tubes were last reported for MOTA-1F at ~119 dpa (3).

RESULTS

Figure 1 shows the total diametral strains measured in each of the tubes, reaching levels as large as 26% ΔD/D without failure. Note that the tubes at the three highest stress levels have developed the 0.33%/dpa maximum diametral deformation rate often observed in pressurized tubes at sufficiently high enough neutron exposures (4-6). Thus, the diametral strain rate has become unresponsive to significant increases in stress level. Even though a volumetric swelling level of ~21% was attained in the absence of stress, the stress-free swelling rate of 0.46%/dpa at the end of the experiment is still far from its maximum possible rate of ~1%/dpa (8), reflecting the relatively low irradiation temperature. Since stress normally accelerates the onset of swelling (7-9), it is expected that the actual stress-affected swelling rates are progressively larger for the pressurized tubes.

DISCUSSION

The slight deviations from completely smooth curves in Figure 1 arise from two contributions. First, the experiment is being conducted over a range of temperatures where the steady-state swelling rate is moderately dependent on temperature, in response to the temperature-dependent operation of the "production bias" concept of freely migrating defect production (10). In this respect, the jump in temperature from 390°C to 433°C at the beginning of the last irradiation segment is considered to be especially significant. Second, there are some minor uncertainties in displacement calculations, with the plotted dpa values representing dpa levels employing calculated neutron exposure levels in some irradiation segments and the measured exposure levels in others. These uncertainties are of no importance, however, in that the creep-swelling coupling coefficients derived from this experiment are defined in terms of the creep rate per dpa divided by the swelling rate per dpa, thus cancelling out any uncertainties in displacement level or rate.

In the traditional U.S. approach for analysis of pressurized tubes, the effect of stress-enhanced swelling is usually ignored, since knowledge of the actual swelling levels requires the destructive examination of the tube and is incompatible with further irradiation and measurement. Thus, the creep rate is overestimated somewhat by considering the stress-enhanced swelling strain as a creep component. Using the traditional approach, we can calculate the creep coefficient associated with the $B_o + D\dot{S}$ creep model, where B_o is the creep compliance and D is the creep-swelling coupling coefficient, relating the stress-normalized creep rate, $\dot{\varepsilon}/\sigma$, to the swelling rate, $\dot{S}$. Table 2 shows that for each tube, B_o~2×10^{-6} MPa^{-1} dpa^{-1} and D~0.6×10^{-2} MPa^{-1}, in excellent agreement with the results of earlier studies on a variety of stainless steels (3,6,11,12).

The attainment of the ~0.33%/dpa diametral deformation rate signals that the creep disappearance phenomenon (13,14) is dominating the experiment, especially in the last irradiation segment. Recent experience with other creep studies has shown that creep disappearance and stress-enhanced swelling appear to be related, such that the effect of stress on swelling cannot be ignored in the analysis.

An effort was made to estimate the stress-enhanced swelling in the pressurized tubes by using the known linear dependence between an applied stress and the resulting creep strain rate in this temperature range. The primary prerequisite for this approach is that the diametral strain rates are below values where the creep disappearance phenomenon is significant, which appears to be the case at the end of MOTA-1G at 153 dpa. As shown in Figure 2, this estimate implied that the swelling at 200 MPa and 153 dpa may be twice as large as that at zero stress. Enhancements of this magnitude have been observed by Dubuisson et al. (9) and Seran et al. (15).

Having estimated those large values of swelling, it is necessary to correct for the resultant decrease in the hoop stress. Unlike irradiation creep, where simultaneous decreases in internal gas pressure and wall thickness compensate almost exactly and hold the hoop stress nearly constant, large swelling levels cause significant decreases in the hoop stress. To analytically simulate constant stress conditions, this non-traditional correction increases the strains incrementally as the irradiation proceeds. The magnitude of the calculated creep strains employing both the stress-enhanced swelling and constant stress assumptions is shown in Figure 3.

Using the strain data from the first seven irradiation sequences only, the creep coefficients at constant stress were calculated for two cases, a) ignoring stress-enhanced swelling and b) including it in the analysis. One facet of the disappearing creep phenomenon observed earlier (16-18) involves a late-term decrease in the creep rate as the swelling rate increases (17,18). As shown in figure 4, ignoring stress-enhanced swelling camouflages the onset of the creep disappearance phenomenon. When stress-enhanced swelling is included, the creep-swelling coupling coefficient declines with increasing stress.

The D-coefficient is actually declining with increasing swelling rate rather than directly with increasing stress. This becomes more obvious in Figure 5, which presents the average D-coefficient as a function of average swelling rate for the first seven irradiation segments, as well as the average D-coefficients calculated for three of the last four individual irradiation segments. Note that these are average D-coefficients and, therefore, the instantaneous coefficients at the end of any irradiation sequence are even lower.

Since most fusion applications will involve stress levels that are much lower than explored in this experiment, it is anticipated that creep rates will diverge significantly from those predicted using the values determined in this experiment. A similar problem has been observed in LMR fuel pins (17). The difficulties associated with application of these data to low-stress, high-swelling situations is discussed elsewhere along with guidelines on how to translate these data for use in such situations (18).

CONCLUSIONS

PCA in the 20% cold-worked condition can survive without failure during fast neutron irradiation to very large stress levels and to very large swelling levels at ~400°C. As swelling becomes significant, however, its influence requires that several non-traditional methods be employed in the analysis of the strain data. The derived creep coefficients also show that the creep rate loses its responsiveness to stress and declines as the swelling rate increases. Application of these data to low stress fusion applications is not completely straightforward and requires more study.

ACKNOWLEDGEMENTS

This work was sponsored by the U.S. Department of Energy under two contracts, DE-AC06-76RLO 1830 with Pacific Northwest Laboratory (operated by Battelle Memorial Institute for the U.S. Department of Energy) and DE-FG06-89ER-75522 with the Northwest College and University Association for Science. The assistance of Jill Walters in preparing the manuscript is gratefully acknowledged.

References

1. F.A. Garner, H.L. Heinisch, R.L. Simons and F.M. Mann, Radiation Effects and Defects in Solids, 113 (1990) 229-255.

2. E.R. Gilbert and B.A. Chin, in: Effects of Radiation on Materials: Tenth Conference, ASTM STP 725, 1981, pp. 665-679.

3. M.B. Toloczko, F.A. Garner, and C.R. Eiholzer, J. Nucl. Mater. 191-194 (1992) 803-807.

4. D.L. Porter and F.A. Garner, J. Nucl. Mater. 159 (1988) 114-121.

5. F.A. Garner and M.B. Toloczko, in: Fusion Reactor Materials Semiannual Progress Report DOE/ER-0313/12 (1992) pp. 145-147.

6. F.A. Garner, M.B. Toloczko and R.J. Puigh, ibid, pp. 148-162.

7. F.A. Garner, E.R. Gilbert and D.L. Porter, in: Effects of Radiation on Materials: Tenth Conference, ASTM STP 725, 1981, pp. 680-697.

8. D.L. Porter, M.L. Takata and E.L. Wood, J. Nucl. Mater. 116 (1983) 272-276.

9. P. Dubuisson, A. Maillard, C. Deladande, D. Gilbon, J.L. Seran in: Effects of Radiation on Materials: Fifteenth International Symposium, ASTM STP 1125, 1992, pp. 995-1014.

10. C.H. Woo, B.N. Singh and F.A. Garner, J. Nucl. Mater. 191-192 (1992) 1224-1228.

11. F.A. Garner and D.L. Porter, J. Nucl. Mater. 155-157 (1988) 1006-1013.

12. D.L. Porter, G. D. Hudman, and F.A. Garner, J. Nucl. Mater. 179-181 (1991) 581-584.

13. C.H. Woo and F.A. Garner, J. Nucl. Mater. 191-194 (1992) 1309-1312.

14. C.H. Woo, F.A. Garner, and R.A. Holt, in: Effects of Radiation on Materials: Sixteenth International Symposium, ASTM STP 1175, 1993, (in press).

15. J.L. Seran, H. Touran, A. Maillard, P. Dubuisson, J.P. Hugot, E. Le Boulbin, P. Blanchard and M. Pelletier, in: Effects of Radiation on Materials: Fourteenth International Symposium, ASTM STP 1146, 1990, pp. 739-752.

16. F.A. Garner, D.L. Porter and B.J. Makenas, J. Nucl. Mater. 148 (1987) 279-287.

17. F.A. Garner and M.B. Toloczko, J. Nucl. Mater. (in press).

18. F.A. Garner, M.B. Toloczko and C.H. Woo, presented at this conference.

FIGURE CAPTIONS

1) Total diametral strains observed in 20% cold-worked PCA tubes at ~400°C and hoop stress levels varying from 0 to 178 MPa. The swelling of the unstressed tube at 178 MPa is 21%.

2) Calculated estimate of stress-enhanced swelling in the first seven irradiation segments, assuming that the creep strains are proportional to the stress level. Extrapolation to 176 dpa yields 35-40% swelling at 200 MPa.

3) Midwall creep strains calculated for both the stress-insensitive swelling and stress-enhanced swelling cases. Large levels of swelling also decrease the stress level in the tube wall and a correction to constant stress must be made.

4) Average creep coefficients vs. hoop stress derived from the first seven irradiation segments for both the stress-insensitive swelling and stress-enhanced swelling cases.

5) Average creep-swelling coupling coefficients vs. average swelling rate, calculated for the first seven irradiation segments, and also for each of the MOTA 1E, 1F, and 1G segments.

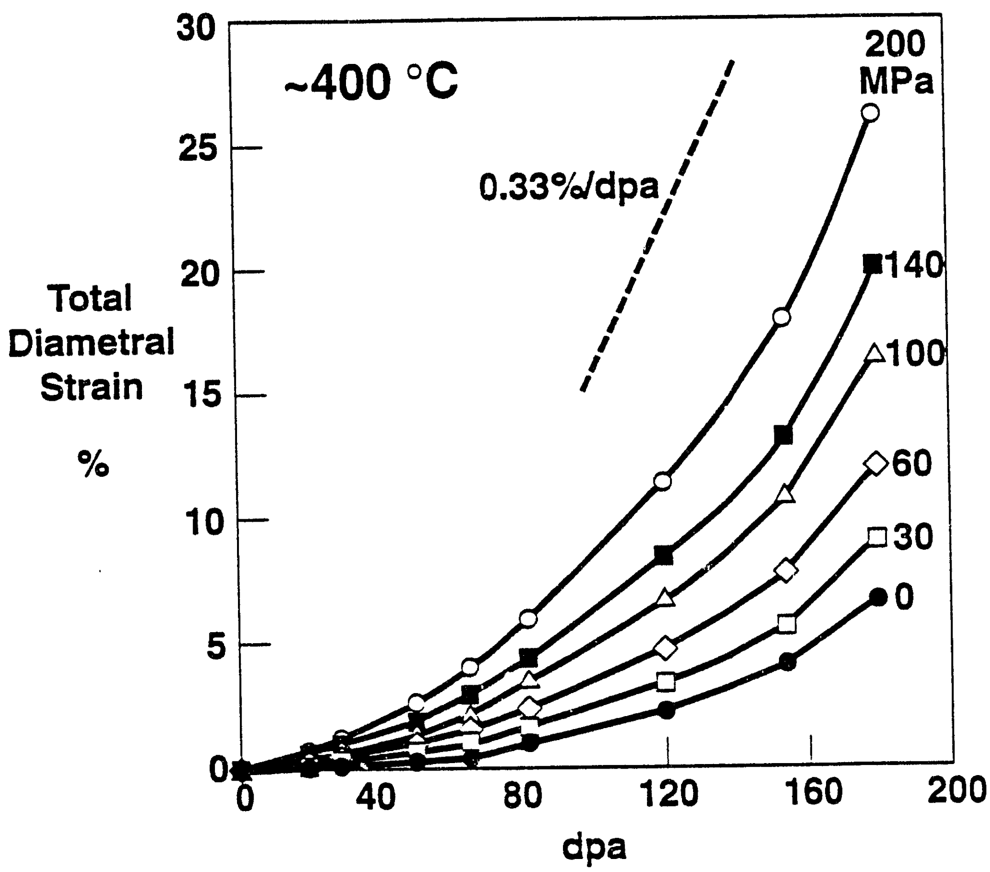

Figure 1. Total diametral strains observed in 20% cold-worked PCA tubes at ~400°C and hoop stress levels varying from 0 to 200 MPa. The swelling of the unstressed tube at 178 dpa is 21%.

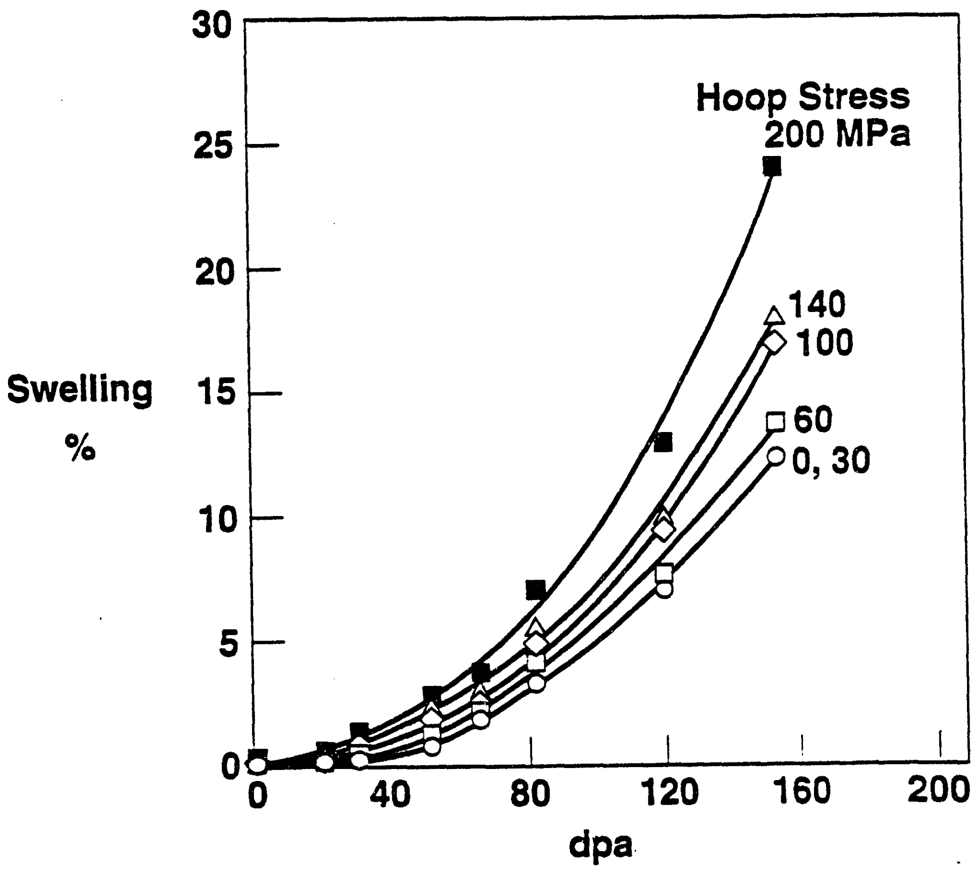

Figure 2. Calculated estimate of stress-enhanced swelling in the first seven irradiation segments, assuming that the creep strains are proportional to the stress level. Extrapolation to 178 dpa yields 35-40% swelling at 200 MPa.

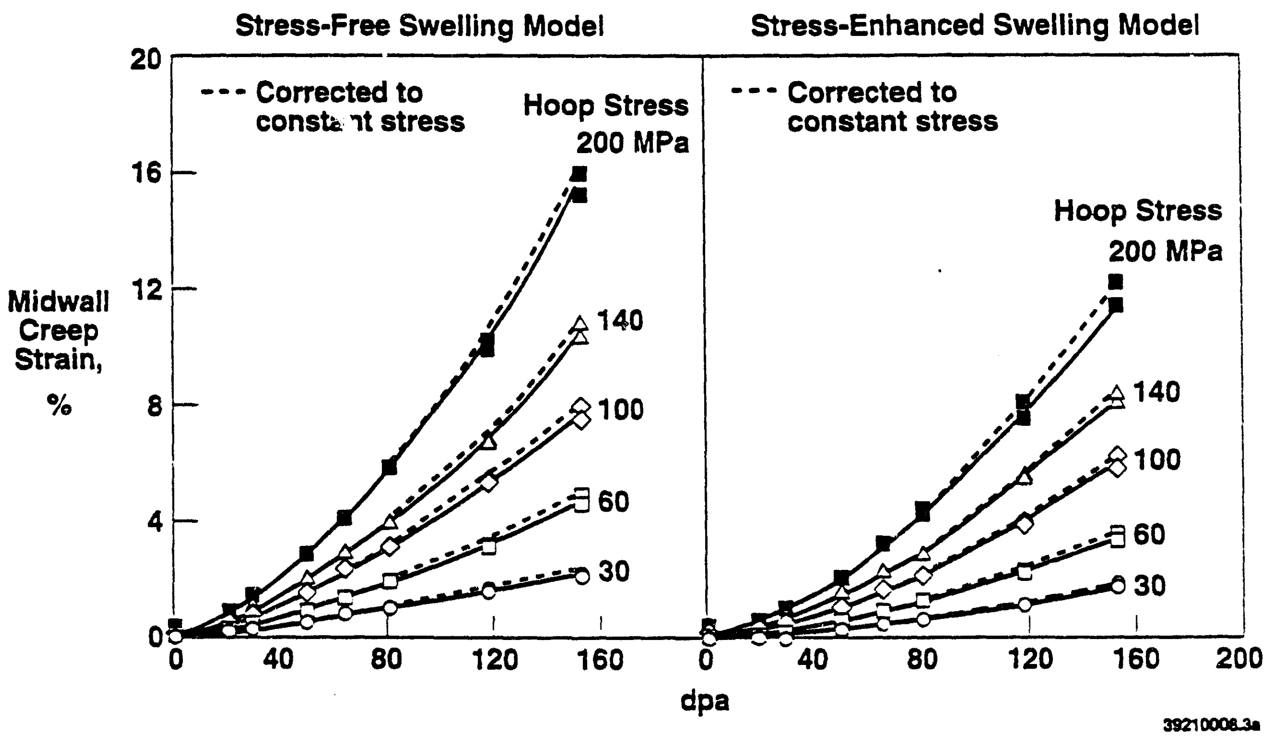

Figure 3. Midwall creep strains calculated for both the stress-insensitive swelling and stress-enhanced swelling cases. Large levels of swelling also decrease the stress level in the tube wall and a correction to constant stress must be made.

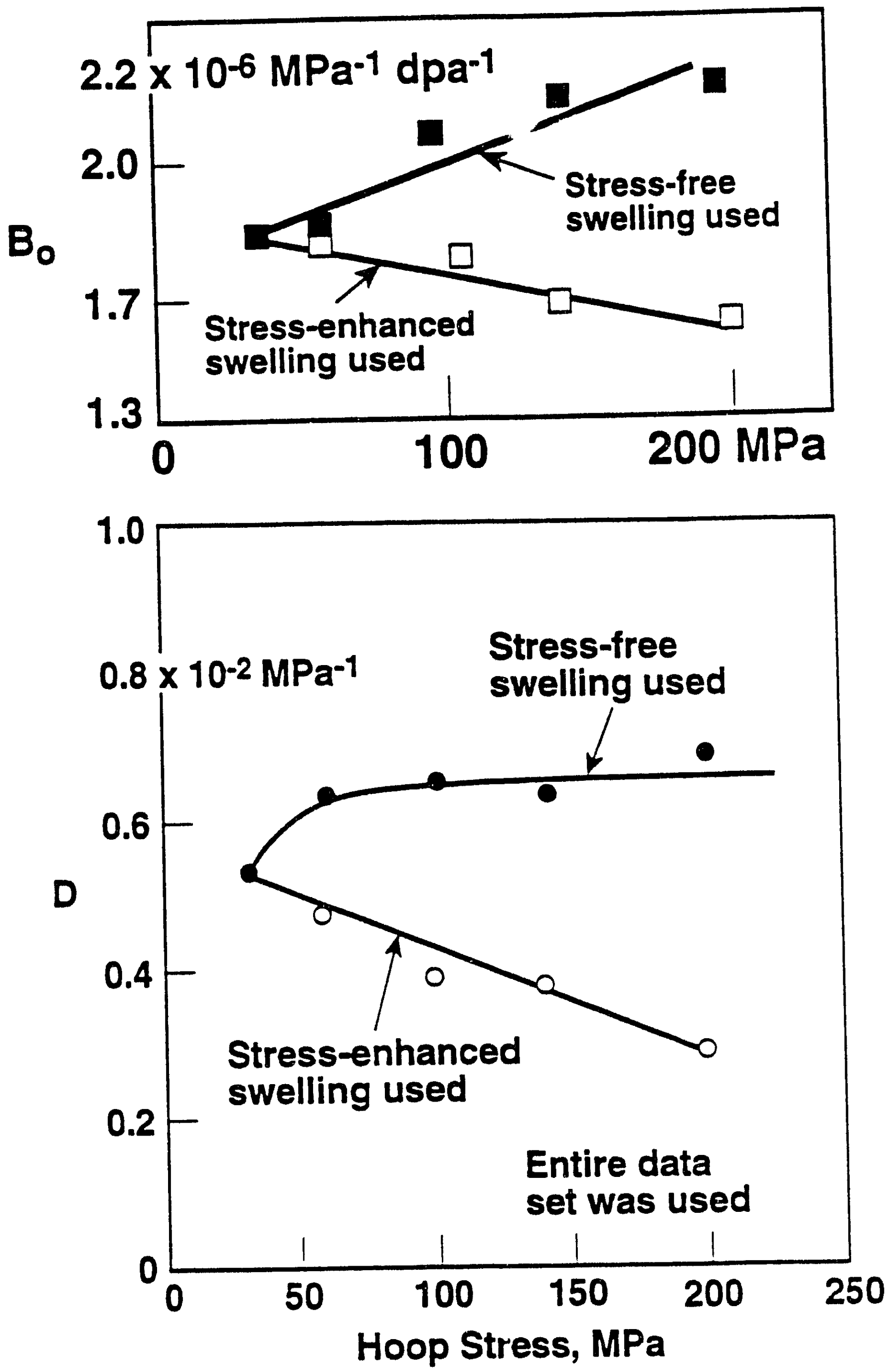

Figure 4. Average creep coefficients vs. hoop stress derived from the first seven irradiation segments for both the stress-insensitive swelling and stress-enhanced swelling cases.

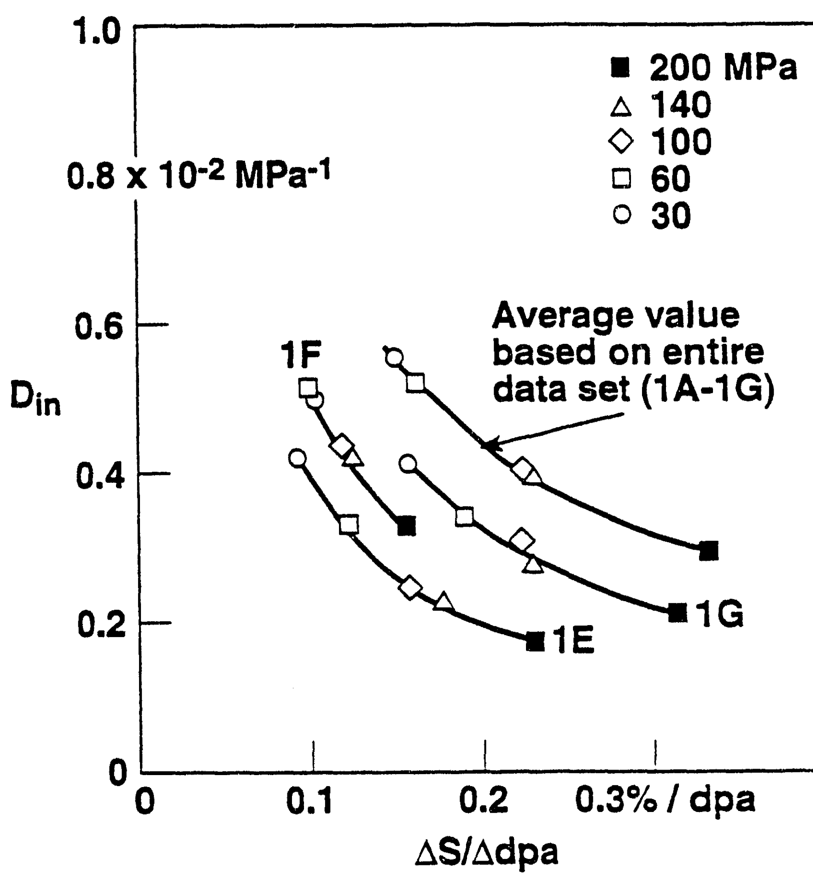

Figure 5. Average creep-swelling coupling coefficients vs. average swelling rate, calculated for the first seven irradiation segments, and also for each of the MOTA 1E, 1F, and 1G segments.

Table 1 Irradiation History of Pressurized Tubes

MOTA	TEMPERATURE, °C
1A	405
1B	401
1C	396
1D	386
1E	384
1F	386
1G	390
2B	433

Table 2. Average creep coefficients derived over the entire interval of 0 to 178 dpa, assuming that stress does not affect swelling.

Stress Level MPa	D MPa^{-1}	B_o MPa^{-1} dpa^{-1}
30	0.58×10^{-2}	1.7×10^{-6}
60	0.53×10^{-2}	2.0×10^{-6}
100	0.57×10^{-2}	2.2×10^{-6}
140	0.54×10^{-2}	2.3×10^{-6}
200	0.57×10^{-2}	2.3×10^{-6}

DATE FILMED

2/8/94

END